GEOMAGNETIC ANOMALOUS SIGNAL IDENTIFICATION PRIOR TO THE MW7.0 EARTHQUAKE GENERATION IN THE COASTAL ZONE OF SAMOS ISLAND-GREECE, ON OCTOBER 30, 2020

DRAGOȘ A. STĂNICĂ

E-mail address (armand@gedin.ro).
Electromagnetism and Lithosphere Dynamics Department, Institute of Geodynamics of the Romanian Academy, 19–21 Jean Louis Calderon Str., R-020032 Bucharest, Romania.

A strong earthquake of Mw7.0 struck the coastal zone of Samos Island, Aegean Sea, on October 30, 2020, at 11:51 UTC. This earthquake was felt on a wide area including Athens (270km far) and city of Heraklion-Crete (at 320km), causing over 120 deaths and a lot of damages on buildings and infrastructures, mainly in Samos Island and Izmir (Turkey). With the aim to identify the geomagnetic anomalous signal before the onset of this earthquake, the data collected on the interval September 16 – October 31, 2020 at the geomagnetic observatories Pedeli (PEG)-Greece and Panagjurishte (PAG)-Bulgaria are retrospectively analysed using the polarization parameter (BPOL) with its standard deviation (SD) and, the strain effect–related to geomagnetic signal identification. Further on, a statistical analysis based on a standardized random variable equation was applied for the following two particular cases: a) to assess on the both geomagnetic time series BPOL*(PEG) and BPOL*(PAG) the anomalous signals related to Mw7.0 earthquake; b) to differentiate transient local anomalies associated with this earthquake from the internal and external parts of the geomagnetic field, taking the PEG Observatory as reference. Finally, on the BPOL*(PEG-PAG) time series, carried out on the interval October 1–31, 2020, a very clear anomaly of maximum, of about 1.17SD, was identified on October 27, with 3days before the onset of Mw7.0 earthquake.

Keywords: geomagnetic anomalous signal; Mw7.0 earthquake; (PEG)–Greece and (PAG)-Bulgaria geomagnetic data; BPOL*(PEG); BPOL*(PAG) and BPOL*(PEG-PAG) time series.

1. INTRODUCTION

The terrestrial and satellite studies carried out in the last years, related to the pre-earthquakes anomalous signature in the Earth's lithosphere and ionosphere, have shown that in both cases, these may be identified in various forms, such as:

Electromagnetic/geomagnetic signature generated by the earthquakes foci, as the Very-Low Frequency (VLF)/Low Frequency (LF) radio network signals emphasized as the earthquake precursors (Biagi *et al*., 2011); the pulse azimuth effect as it was seen in the induction coil magnetometers and its possible association with the earthquake (Dunson *et al*., 2011); global variation of the Ultra-Low Frequency (ULF) geomagnetic field using one observatory as reference (Hayakava *et al*., 2011; Hattori *et al*., 2013); geomagnetic diurnal variation associated with the 2011, Mw9.0 Tohoku earthquake (Han *et al*., 2015); retrospective investigation of geophysical data associated with Ms8.0 Wenchuan earthquake, China (Huang *et al*., 2011); anomalous pre-seismic behavior of the electromagnetic normalized functions related to the Vrancea intermediate depth earthquakes, Romania (Stanică and Stanică, 2011); long-range anomalous effect related to M9 Great Tohoku earthquake (Stanică *et al*., 2015); pre-seismic geomagnetic anomalous signature due to the Mw7.0 earthquake generated in the northern coastal zone of Samos Island–Greece (Stănică and Stănică, 2021).

The electric conductivity changes that in the conditions imposed by geophysical properties may create internal current concentration, flowing through the fluids or the surrounding rocks, what gives rise the anomalous geomagnetic signals due to some factors such as: a possible correlation between crustal conductivity variation and geodynamic process (Bataleva *et al*., 2013);

structural heterogeneity in the mega-thrust zone and mechanism of the 2011 Tohoku-oki earthquake Mw 9.0 (Zao *et al*., 2011); magnetic index based on the external part of vertical geomagnetic variation (Ernst *et al*., 2010); natural time analysis (Sarlis *et al*., 2018 and, 2020); self–organized critically and earthquake predictibility (Varotsos *et al*., 2020); advances in multi-parametric, time-dependent assessment of seismic hazard and earthquakes forecast (Tramutoli and Vallianatos, 2020).

Plasma turbulence in ionosphere prior to earthquakes as possible precursor to the March 11, 2011, Japan earthquake due to the ionospheric perturbation as it was seen as sub ionospheric VLF/LF propagation (Hayakawa *et al*., 2012); studies of the electromagnetic variation in extra low frequency (ELF) range over the Sichuan region prior the May 12, 2008 earthquake (Błęcki *et al*.2010); some remarks on the DEMETER registrations (Błęcki *et al*., 2011); atmosphere-ionosphere response to the M9 Tohoku earthquake revealed by multi-instrument space born and ground based observations (Ouzounov *et al*., 2011); unexpected events recorded by the ionospheric satellite DEMETER (Parrot, *et al*., 2015).

Further on, the main purpose of this paper is to obtain, by using the specific ground-based theoretical concepts, a pre-seismic geomagnetic signature due to the Mw7.0 earthquake generated in the northern coastal zone of Samos Island-Greece. Consequently, in order to carry out the above mentioned information, the data collected via internet (htttp:www.intermagnet.org), from the geomagnetic observatories Pedeli (PEG)–Greece and Panagjurishte (PAG)–Bulgaria, are used to draw up the following time series: BPOL(PEG), BPOL(PAG), ABS BOPL*(PEG), ABS BPOL*(PAG) and ABS BPOL*(PEG–PAG).

2. MATERIALS AND METHODS

2.1. EARTHQUAKE LOCATION AND SEISMICITY

According to the data offered by the Euro Mediterranean Seismic Centre (http://www.emsc-csem.org), on October 30, 2020,11:51 UTC, an earthquake of Mw7.0 that was generated in the Aegean Sea, at about 10km depth, struck the northern coastal zone of Samos Island, Greece, see the map in Fig. 1. It was felt on a wide area, including Athens, causing 120 deaths and damages on buildings and infrastructures in Samos Island and Izmir town in Turkey. To have an idea about the circumstances regarding the Mw7.0 earthquake occurrence, on the above-mentioned map, the seismicity from the previously 7 days in the area is presented by means of red, brown and yellow circles in Fig. 1. It is also to mention, that for the both geomagnetic observatories Pedeli (PEG)-Greece and Panagjurishte (PAG)-Bulgaria the data were obtained, via internet (http://www.intermagnet.org).

2.2. BASIC THEORETICAL CONCEPTS

The main scope of this paper is to show how a seismic activity could be reflected in the geomagnetic field variations, by applying an appropriate methodology able to emphasize a pre-earthquake anomalous signature. Consequently, some theoretical concepts concerning the earthquake generation mechanism had to be taken into consideration, as following: piezomagnetic, magneto-hydrodynamic and electrokinetic effects (Varotsos, 2005).

To identify a possible pre-seismic anomalous signature related to Mw7.0 earthquake, the Rel. (1) given by Morgunov and Malzev, 2007 was used to emphasize:

– The range effect of the strain for pre-seismic geomagnetic signal identification, due to the above- mentioned earthquake using Relation (1):

$$R(km) = 10^{0.5M-0.27}, \quad (1)$$

where:

R is distance between Mw7.0 earthquake and the both geomagnetic observatories;

M is earthquake magnitude.

In conformity with Relation (1), the range effect of the strain-related to Mw7.0 earthquake is R ~ 1700km and the epicentral distances for the two geomagnetic observatories are:

R ~ 270km for PEG – Greece and, respectively, R ~ 540km for PAG – Bulgaria (see Fig. 2).

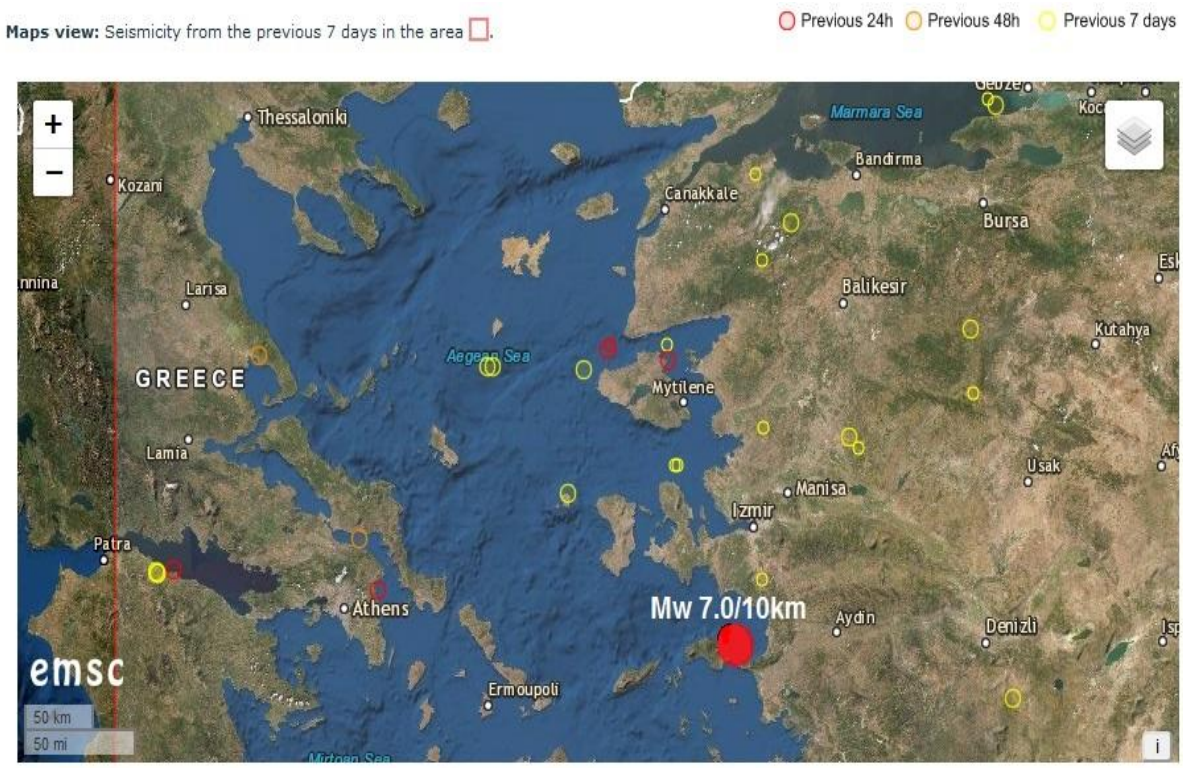

Fig.1. Map with the Mw7.0 earthquake placement (red full circle) and the previous 24h, 48h and 7days seismicity (red, brown and yellow empty circles); Mw7.0/10km is earthquake magnitude/depth, according to the Euro- Mediterranean Seismic Centre (http://www.emsc-csem.org).

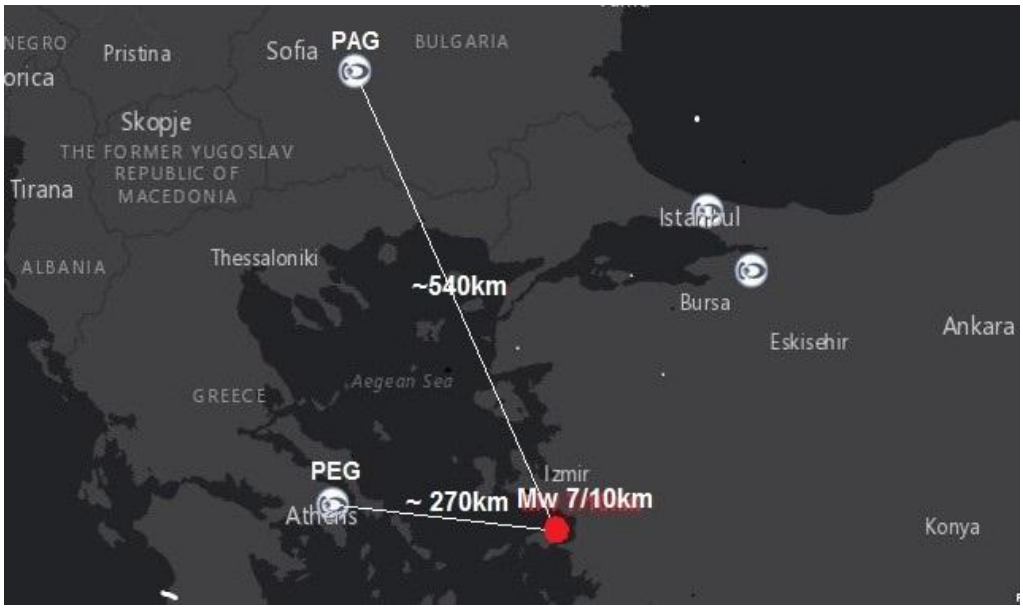

Fig.2. Map with the Mw7/10km earthquake (red full circle) and the placements of the geomagnetic observatories PEG (Greece) and PAG (Bulgaria), according to (http://www.intermagnet.org); 540km and 270km are distances between the observatories and earthquake location.

As the distances between the PEG and PAG geomagnetic observatories and the location of the Mw7.0 earthquake is less than 1700km, the conditions to identify a pre-earthquake geomagnetic anomalous signature is fulfilled.

2.3. GEOMAGNETIC DATA COLLECTIONS, PROCESSING AND ANALYSIS

The geomagnetic data Bx, By and Bz where obtained on the interval September 16 – October 31, 2020, via internet (http://www.intermagnet.org), from the both geomagnetic observatories (PEG)-Greece and (PAG)-Bulgaria are used for the following three purposes:

a) To carry out the time series of the Polarization Parameter (BPOL) and its Standard Deviation (SD) for the geomagnetic
b) observatories (PAG)-Bulgaria and (PEG)-Greece, using Rel. (2):

$$\mathrm{BPOL(f)} = \frac{\mathrm{Bz(f)}}{\sqrt{[\mathrm{Bx^2(f)+By^2(f)}]}}, \quad (2)$$

where:

Bx(f), By(f) and Bz(f) are horizontal and vertical components of the geomagnetic field in (μT), f is frequency in (Hz);

c) To identify a possible pre-seismic geomagnetic signal, associated with the Mw7.0 earthquake, using a statistical analysis based on the Rel. (3):

$$\mathrm{BPOL^*(PAG)} = \frac{\mathrm{A-B}}{\mathrm{C}}, \quad (3)$$

where:

A is the values of BPOL obtained on the interval September 16–October 31, 2020;

B is 30 days running average of the BPOL, on the consecutive days, before the specific day;

C is as B, using SD; BPOL*(PAG) time series represent the threshold for anomaly using SD;

Similar relation is applied for BPOL* (PEG).

d) To emphasize the geomagnetic pre-seismic signal generated by the Mw7.0 earthquake, a statistical analysis is applied taking the PEG observatory as reference, using the Rel. (4):

$$\mathrm{BPOL^*(PEG-PAG)} = \frac{\mathrm{X-Y}}{\mathrm{W}}, \quad (4)$$

where:

X is difference between BPOL (PEG) and BPOL (PAG) for a specific day, on the interval October 01–31, 2020;

Y is 30 days running average of BPOL (PEG) – BPOL(PAG) before a specific day;

W is 30 days running average of SD (PEG) – SD (PAG) before a specific day.

BPOL*(PEG-PAG) time series emphasizes the threshold for anomaly using SD.

3. RESULTS AND DISCUSSIONS

After the necessary information concerning the range effect of the strain for anomalous geomagnetic signal identification, prior to the Mw7.0 earthquake, was established with Rel. (1), the time series of the polarization parameter (BPOL) and its standard deviation (SD) for PEG and PAG observatories are obtained using Rel. (2), further on a statistical analysis based on the standardized random variable equation was applied for:

– to identify anomalous geomagnetic signal triggered by the Mw7.0 earthquake using Rel. (3);
– to separate the above anomalous signal from the ionospheric and terrestrial geomagnetic field variation with Rel. (4).

Further on, the geomagnetic time series with pre-seismic geomagnetic signatures related to Mw7.0 earthquake are presented as:

Tables 1, 2, 3 and associated Figures 3–7.

Table 1

Date	BPOL(PAG) – Bulgaria	SD(PAG) – Bulgaria	BPOL(PEG) – Greece	SD(PEG) – Greece
16.09.2020	1.728206184	0.000978078	1.424268224	0.000480273
17.09.2020	1.727949154	0.000707909	1.424268224	0.000480273
18.09.2020	1.727665245	0.000601124	1.423820416	0.000555479
19.09.2020	1.727872214	0.00047403	1.42424691	0.000224552
20.09.2020	1.72790812	0.000615434	1.424028612	0.000462361
21.09.2020	1.727239043	0.000566311	1.423532018	0.000388518
22.09.2020	1.727489549	0.000450133	1.424194957	0.000377134
23.09.2020	1.727572231	0.000448138	1.424532882	0.000561538
24.09.2020	1.729145038	0.001324106	1.42528207	0.000852687
25.09.2020	1.728618491	0.000582868	1.425029452	0.000521984
26.09.2020	1.729297548	0.001092545	1.425443764	0.000613703
27.09.2020	1.729265273	0.000719073	1.425564878	0.000591838
28.09.2020	1.730142353	0.000943128	1.426318924	0.000631849
29.09.2020	1.729675632	0.000696668	1.425560352	0.000495936
30.09.2020	1.729632179	0.00043253	1.425429217	0.000904029
01.10.2020	1.729389548	0.000292718	1.425390622	0.000605583
02.10.2020	1.729262542	0.000401773	1.425490941	0.000373357
03.10.2020	1.728969513	0.00046823	1.425134244	0.000448601
04.10.2020	1.728841092	0.000360369	1.424999889	0.00031378
05.10.2020	1.728454784	0.000779569	1.425247275	0.000322574
06.10.2020	1.728591831	0.000465309	1.424616069	0.000439186
07.10.2020	1.727749048	0.000326029	1.424278729	0.000435614
08.10.2020	1.728371712	0.000160266	1.42463355	0.000163549
09.10.2020	1.728021376	0.000266594	1.424347437	0.000301583
10.10.2020	1.72786369	0.000201086	1.424255983	0.000308808
11.10.2020	1.727133268	0.000725644	1.423849602	0.000583192
12.10.2020	1.727640968	0.000635905	1.423906898	0.000617693
13.10.2020	1.72737886	0.000572194	1.423817738	0.000529036
14.10.2020	1.727501883	0.000516294	1.424033189	0.000391467
15.10.2020	1.727686096	0.000230163	1.424068309	0.000269845
16.10.2020	1.727336041	0.000808827	1.424023200	0.000588044
17.10.2020	1.728041544	0.000634863	1.424323328	0.000452589
18.10.2020	1.727568886	0.000610474	1.424164711	0.00047207
19.10.2020	1.727887368	0.000260695	1.424444378	0.00036156
20.10.2020	1.728139075	0.000160241	1.424481837	0.000233789
21.10.2020	1.727433193	0.000548663	1.424406987	0.000564173
22.10.2020	1.728024628	0.000470382	1.424374184	0.000547508
23.10.2020	1.728181751	0.000403844	1.424112818	0.000736348
24.10.2020	1.729070007	0.000758965	1.425578485	0.000571983
25.10.2020	1.72902822	0.000699202	1.42552076	0.000616209
26.10.2020	1.72927175	0.000873015	1.425481414	0.000572894
27.10.2020	1.729575677	0.000707728	1.425298827	0.000346808
28.10.2020	1.72956237	0.000767979	1.425606332	0.000552986
29.10.2020	1.729396856	0.00074265	1.425577937	0.00054393
30.10.2020	1.729206155	0.000326233	1.425139142	0.00033053
31.10.2020	1.729252443	0.000911556	1.425326529	0.000493146

BPOL and SD time series for the PAG and PEG observatories, carried out with Rel. (2) on the interval September 16 – October 31.2020, are used to draw up Figs.3 and 4.

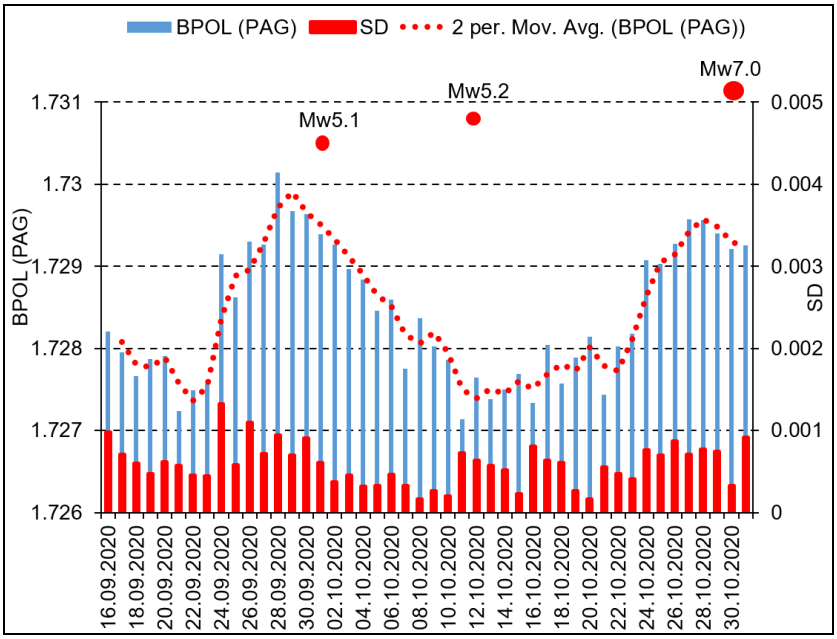

Fig. 3. BPOL (PAG) and standard deviation (SD) time series obtained on the interval September 16 – October 31, 2020; vertical blue and red bars are BPOL and SD; red circles (Mw5.1 and Mw5.2) are earthquakes generated in Aegean Sea (Crete Island) on October 01 and 12, before the Mw7.0 earthquake on October 30 (red circle); red dotted line is 2 days' average values of the BPOL(PAG).

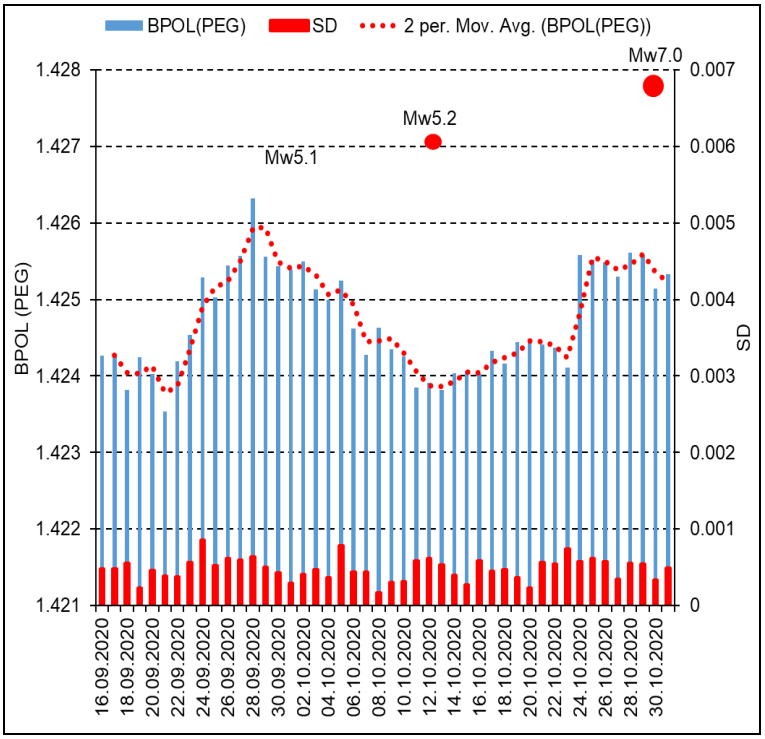

Fig. 4. BPOL (PEG) and standard deviation (SD) time series carried out on the interval September 16 – November 30, 2020; vertical blue and red bars are BPOL and SD; red circles (Mw5.1 and Mw5.2) are earthquakes generated in Aegean Sea (Crete Island) on October 01 and 12, before the Mw7.0 earthquake on October 30 (red circle); red dotted line is 2 days' average values of the BPOL(PEG).

Table 2

DATE	ABS BPOL*(PAG)	ABS BPOL*(PEG)	Earthquake Magnitude/Depth
01.10.2020	1.185651215	1.217422762	5.1/154km
02.10.2020	0.939002686	1.299036095	
03.10.2020	0.420110389	0.425093186	
04.10.2020	0.111002104	0.024805151	
05.10.2020	0.557966011	0.372499721	
06.10.2020	0.420528605	1.018026669	
07.10.2020	1.869152308	1.797023645	
08.10.2020	0.944137901	1.118856672	
09.10.2020	1.626005668	1.765469386	
10.10.2020	1.986225008	1.968939306	
11.10.2020	3.384408765	2.823749284	
12.10.2020	2.241695186	2.469698556	5.2/11km
13.10.2020	2.579210841	2.412428033	
14.10.2020	2.058789171	1.582609634	
15.10.2020	1.391036009	1.292288754	
16.10.2020	2.079313312	1.217550537	
17.10.2020	0.028200822	0.279172149	
18.10.2020	0.91253746	0.458196824	
19.10.2020	0.01906347	0.31374333	
20.10.2020	0.721215654	0.480617377	
21.10.2020	0.823436281	0.465165155	
22.10.2020	0.693369629	0.410788948	
23.10.2020	0.98462077	0.225384837	
24.10.2020	2.868557164	3.027819662	
25.10.2020	2.458934977	2.624443474	
26.10.2020	2.616168572	2.271219212	
27.10.2020	2.864817583	1.693530465	
28.10.2020	2.581362962	2.200731205	
29.10.2020	1.969434533	1.889225095	
30.10.2020	1.370049129	0.756805652	7/10km
31.10.2020	1.260932911	0.982937016	

ABS BPOL(PAG) and ABS BPOL*(PEG) time series obtained with Rel. (3), on the interval October 01-31.2020 for the both geomagnetic observatories, are used to draw up Figs. 5 and 6.*

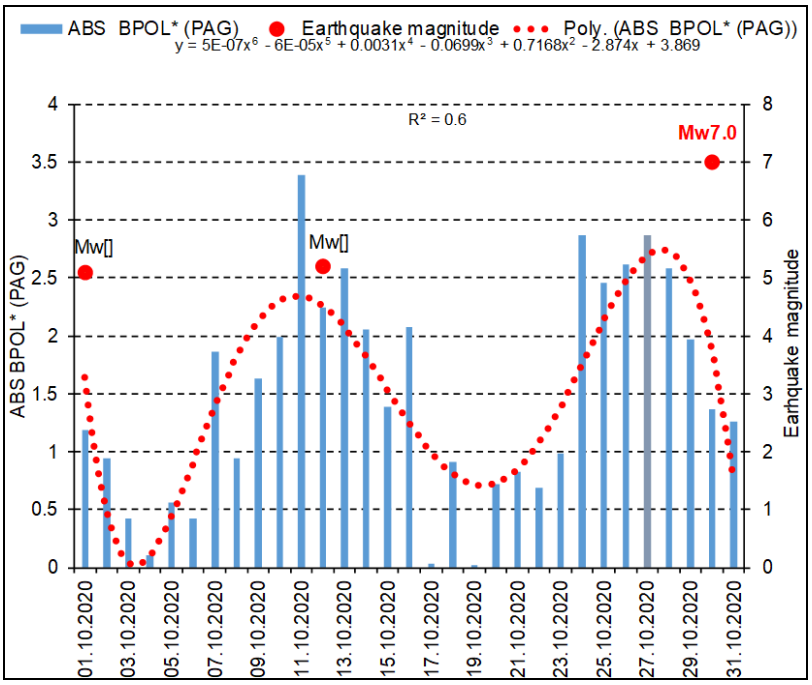

Fig. 5. ABS BPOL*(PAG) time series (blue bars) carried out on the interval October 1–31, 2020; red dotted line delineates a polynomial regression of order 6 (y); R^2 is root-mean-square value; ABS means Absolute Value; red full circles are earthquakes; vertical red arrow on October 27 emphasizes a pre-seismic anomalous signal related to Mw7.0 earthquake.

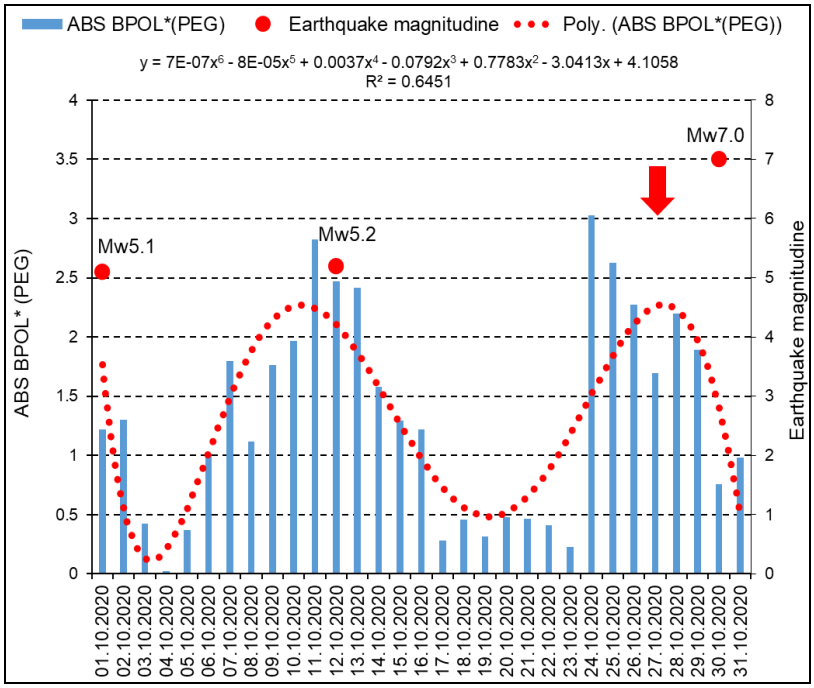

Fig. 6. ABS BPOL*(PEG) time series (blue bars) carried out on the interval October 1–31, 2020; red dotted line delineates a polynomial regression of order 6 (y); R^2 is root-mean-square value; ABS means Absolute Value; red full circles are earthquakes; vertical red arrow on October 27 emphasizes a pre-seismic anomalous signal related to Mw7.0 earthquake.

Table 3

DATE	ABS BPOL*(PEG)	ABS BPOL*(PAG)	ABS POL*(PEG-PAG)	Eq.Magnitude/Depth
01.10.2020	1.217422762	1.185651215	0.031771548	
02.10.2020	1.299036095	0.939002686	0.360033409	
03.10.2020	0.425093185	0.420110389	0.004982797	
04.10.2020	0.024805151	0.111002104	0.086196953	
05.10.2020	0.372499721	0.557966011	0.185466291	
06.10.2020	1.018026669	0.420528605	0.597498064	
07.10.2020	1.797023645	1.869152308	0.072128663	
08.10.2020	1.118856672	0.944137901	0.174718771	
09.10.2020	1.765469386	1.626005668	0.139463718	
10.10.2020	1.968939306	1.986225008	0.017285702	
11.10.2020	2.823749284	3.384408765	0.560659480	
12.10.2020	2.469698556	2.241695186	0.228003369	
13.10.2020	2.412428033	2.579210841	0.166782809	
14.10.2020	1.582609634	2.058789171	0.476179537	
15.10.2020	1.292288754	1.391036009	0.098747255	
16.10.2020	1.217550537	2.079313312	0.861762774	
17.10.2020	0.279172149	0.028200822	0.250971327	
18.10.2020	0.458196824	0.912537460	0.454340636	
19.10.2020	0.31374333	0.019063470	0.294679860	
20.10.2020	0.480617377	0.721215654	0.240598277	
21.10.2020	0.465165155	0.823436281	0.358271127	
22.10.2020	0.410788948	0.693369629	0.282580681	
23.10.2020	0.225384837	0.984620770	0.759235932	
24.10.2020	3.027819662	2.868557164	0.159262497	
25.10.2020	2.624443474	2.458934977	0.165508498	
26.10.2020	2.271219212	2.616168572	0.344949360	
27.10.2020	1.693530465	2.864817583	1.171287118	
28.10.2020	2.200731205	2.581362962	0.380631757	
29.10.2020	1.889225095	1.969434533	0.080209438	
30.10.2020	0.756805652	1.370049129	0.613243478	**7.0/10km**
31.10.2020	0.982937016	1.260932911	0.277995896	

ABS BPOL(PEG), ABS BPOL*(PAG) and ABS*(PEG-PAG) time series, obtained on the interval October 01-31.2020 for the both geomagnetic observatories with Rel. (4), are used to draw up Fig. 7.*

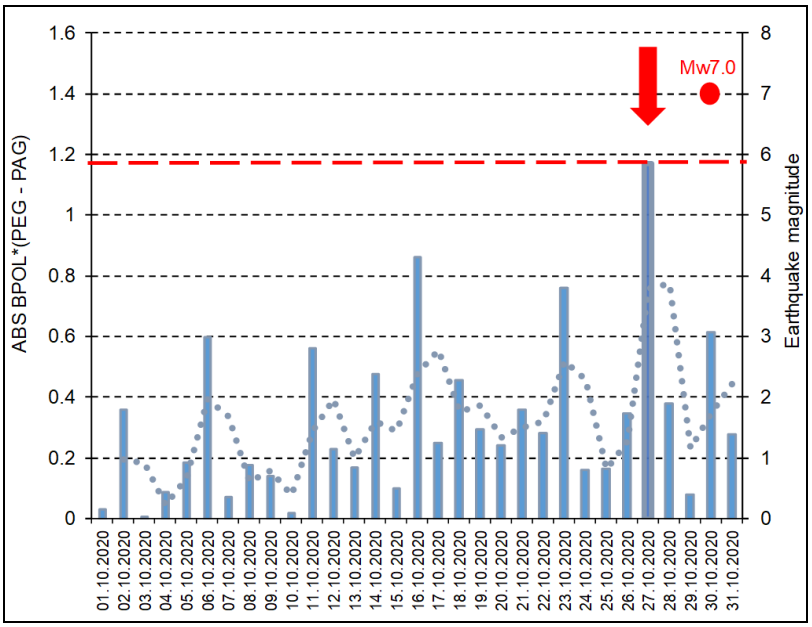

Fig. 7. ABS BPOL*(PEG-PAG) time series (blue bars) carried out on the interval October 1–31, 2020; blue dotted line is 2 days' average value of this time series; red full circle is Mw7.0 earthquake; red dashed line placed at about 1.17 on October 27, delineates the threshold for anomaly using SD; vertical red arrow indicates on October 27, 2020 a pre-seismic geomagnetic anomalous signal associated with the Mw7.0 earthquake.

4. CONCLUSIONS

In this study, the data have been collected from the geomagnetic observatories Panagjurishte (PAG)-Bulgaria and Pedeli (PEG)-Greece, via (http://www.intermagnet.org), and retrospectively analyzed applying a complex analysis on the following two specific intervals: September 16 – October 31, 2020 and October 1 – October 31, 2020, both of them being used to emphasize a possible pre-seismic geomagnetic anomalous signal related to the Mw7.0 earthquake.

Further on, taking into-account that the range effect of the strain associate to the Mw7.0 earthquake was obtained by using Rel. (1), the necessary information regarding the BPOL(PAG), BPOL(PEG), ABS BPOL*(PAG), ABS BPOL*(PEG) and ABS BPOL*(PEG-PAG) time series have been supplied according to the Relations 2÷4 and, all of them have shown a consistent occurrence of the anomalous signature on October 27, 2020, with 3 days prior to the Mw7.0 earthquake generation, as it was identified in the all geomagnetic time series used and presented in the Tables 1÷3 and Figures 3÷7.

The above-mentioned results lay further support to apply this methodology for the geomagnetic pre-seismic anomalous signals identification, providing a consistent framework for understanding the earthquake generation mechanism, what represents a useful contribution for a better resilience and, consequently, to decrease the catastrophic risks.

Declaration of competing interests

The author declare that he has no known competing financial interests or personal relationships that could have appeared to influence the work reported in this paper.

Data availability

Data will be made available on request.

Special issue statement

This article is associated with the conference EGU General Assembly 2021, online, Aprile 19–30, 2021, EGU21-1078, https://doi.org/10.5194/egusphere-egu21-1078.

Acknowledgements

In this paper, I used the data collected at the two Geomagnetic Observatories located in Panagjurishte (PAG), Bulgaria and Pedeli (PED), Greece, and therefore, I would like to thank the national institutes that support them and INTERMAGNET (http://www.intermagnet.org) for promoting

high standards of magnetic observatory practice. My contentedness to the Euro Mediterranean Seismic Centre (http://www.emsc-csem.org) for using the map with the Mw7.0 and previous 24h, 48h and 7days earthquakes' placement.

REFERENCES

Bataleva, E. A., Batalev, V.Yu., Rubin, K., 2013. On the correlation of crustal conductivity variation and geodynamic processe. Izvestya. Phys Solid Earth 3, 105–113.

Biagi, P.F., Maggipinto, T., Righetti, F., Loiacono, D.D., Schiavulli, L., Ligonzo, T., Ermini, A., Moldovan, I.A., Moldovan, A.S., Buyuksarac, A., Silva, H.G., Bezzeghoud, M., and Contadakis, M.E., 2011. The European VLF/LF radio network to search for earthquake precursors: setting up and natural/man-made disturbances. Nat. Hazards Earth Syst. Sci. 11, 333–341, https://doi.org/10.5194/nhess-11-333-2011.

Błęcki, J., Parrot, M., Wronowski, R., 2010. Studies of the electromagnetic field variations in ELF frequency range registered by DEMETER over the Sichuan region prior the 12 May 2008 earthquake, 2010. International Journal of Remote Sensing, 31, 3615–3629, https://doi.org/10.1080/01431161003727754.

Błęcki, J., Parrot, M., Wronowski, R., 2011. Plasma turbulence in the ionosphere prior to earthquakes, some remarks on the DEMETER registrations, JAES, 41, 450–458, https://doi.org/10.1016/j.jseaes.2010.05.016.

Dunson, J.F., Bleier, T.E., Roth, S., Heraud, J., Alvareez, C.H., Lira, A., 2011. The pulse azimuth effect as seen in induction coil magnetometers located in California and Peru 2007-2010, and its possible association with the earthquake. Nat. Hazard Earth Sys. Sci., 11, 2085–2105, https://doi:org/10.5194/nhess-11-2085-2011.

Ernst, T., Jankovki, J., Nowozinski, K., 2010. A new magnetic index based on the external part of vertical geomagnetic variation. Acta Geophys. 58(6), 963–972, https://doi.org/10.2478/s11600-010-0014-9.

Han, P., Hattori, K., Xu, G., Ashida, R., Chen, C.H., Febriani, F., Yamaguchi, H., 2015. Further investigation of geomagnetic diurnal variation associated with the 2011 off the Pacific coast of Tohoku earthquake (Mw9.0). J. Asian Earth Sciences. 114, 321–326, http://dx.doi.org/10.1016/j.jseaes.2015.02.022.

Hattori, K., Han, P., Huang, Q., 2013. Global variation of the ULF geomagnetic field and detection of anomalous changes at a certain observatory using reference data. Electric Eng. Japan. 182, 9–18, https://doi.org/10.1002/eej.22299.

Hayakawa, M., Hobara, Y., Ohta, K., Hattory, K., 2011. The Ultra-Low-Frequency Magnetic Disturbances Associated with Earthquakes. Earthquake Science, 24, 523–534, https://www.scirp.org http://dx.doi.org/10.1007/s11589-011-0814-2.

Hayakawa, M., Hobara, Y., Yasuda, Y., Yamaguchi, H., Ohta, K., Izutsu, J., Nakamura, T., 2012. Possible precursor to the March 11, 2011, Japan earthquake: Ionospheric perturbation as seen by subionospheric very low frequency/low frequency propagation. Annals of Geophysics 55, 1, 95–99, https://www.annalsof geophysics.eu/ index.php/annals/article/view/5357.

Huang, Q., 2011. Retrospective investigation of geophysical data possibly associated with Ms8.0 Wenchuan earthquake in Sichuan, China. J. Asian Earth Sci. 41, 421–427, https://doi.org/10.1007/s11589-011-0814-2.

Morgunov, V.A., Malzev, S. A., 2007. A multiple fracture model of pre-seismic electromagnetic phenomena. Tectonophysics 431, 61–72. https://doi.org/10.1016/j.tecto.2006.05.030.

Ouzounov, O., Pulinets, S., Romanov., Tsybulya., K., Davidenko, D., Kafatos, M., Taylor, P., 2011. Atmosphere-ionosphere response to the M9 Tohoku earthquake revealed by Joined Satellite and ground observations: Preliminary results. Earthq. Sci. 24, 117–132. https://arxiv.org/ftp/arxiv/papers/1105/1105.2841.pdf.

Parrot, M., Berthelier, J. J., Blecki, J., Brochot J.Y., Hobara, Y., Lagoutte, D., Lebreton, J.P., Němec, F., Onishi, T., Pinçon, J.L., Pisa, D., Santolík, O., Sauvaud, J.A., Slominska, E., 2015. Unexpected events recorded by the ionospheric satellite DEMETER. Survive Geophys 36:483–511, https://doi.org/10.1007/s10712-015-9315-5.

Sarlis, N.V., Skordas, E. S., Varotsos, P. A. Ramirez-Rojas, A., Flores-Maques, E. L., 2018. Natural Time analyses: On the deadly Mexico M8.2earthquake on 7 September 2017, Physica A: Statistical Mechanics and its Application, Elsevier, vol.506, 625–634, http://www.sciencedirect.com/science/article/pii/S0378437118305260,https://doi.org/10.1016/j.physa.2018.04.098.

Sarlis, N.V., Skordas, E.S., Cristopoulos, S.R., Varotsos, P.A., 2020. Natural time analysis: The area under the receiver operating characteristic curve of the order parameter fluctuation minima preceding major earthquakes, Entropy 2020, 22(5), 583. https://doi.org/10.3390/e22050583.

Stănică, D., Stănică, D.A., 2011. Anomalous pre-seismic behavior of the electromagnetic normalized functions related to the intermediate depth earthquakes occured in Vrancea zone, Romania. Nat. Hazard Earth Syst. Sci., 11, 3151–3156. www.nat-hazards-earth-sust-sci.net/11/3151/2011/doi:10.5194/nhess-11-3151-2011.

Stanica, D., A., Stanica, D., Vladimirescu, N., 2015. Long-range anomalous electromagnetic effect related to M9 Great Tohoku earthquake. *Earth Sciences*. Vol. 4, No.1, 31–38, http://www.sciencepublishinggroup.com/j/earth/doi.org/10.11648/j.earth.20150401.13.

Stănică, D., Stănică, D. A. , 2021. Pre-seismic geomagnetic anomalous signature related to the Mw7.0 earthquake generated in the northern coastal zone of Samos island–Greece, on October 30, 2020. EGU General Assembly,

online presentation, 19–30 Apr 2021, EGU21-1078, https://doi.org/10.5194/ egusphere-egu21-1078.

Tramutoli, V., Vallianatos, F., 2020. Advances in Multi-Parametric, Time-Dependent Assessment of Seismic Hazard and Earthquakes Forecast, Annals of Geophysics, Special Issue (t-DASH), 63, 5, PA551, https://doi:10.440/ag-8594.

Varotsos, P.A., 2005. The Physics of Seismic Electric Signals; TERRAPAB, Tokyo, Japan.

Varotsos, P.A., Sarlis, N.V., Skordas, E.S., 2020. Self–organized criticaly and earthquake predictibility: A long-stading questuion in the light natural time analysis, Europhysics Letters (EPL), volume 132, Issue 2, https://iopscience.iop.org/article/10.1209/0295-5075/132/29001/pdf.

Zao, D., Huang, Z., Umino, N., Hasegawa, A., Kanamori, H., 2011. Structural heterogeneity in the mega-thrast zone and mechanism of the 2011 Tohoku-oki earthquake (Mw 9.0). Geophys. Res. Lett., L17308, 5pp,https://authors. library.caltech.edu/26594/1/zhao 2011p15956geophys_Res_Lett.pdf, doi:10.1029/2011GL048408.